Electronic Journal of Biotechnology 18 (2015) 480–485

HOSTED BY

Contents lists available at ScienceDirect

Electronic Journal of Biotechnology

Research Article

Topological analysis of carbon flux during multi-stress adaptation in *Halomonas* sp. AAD12

Hilal Mangaoglu Yoruk, Nihat Alpagu Sayar *

Department of Bioengineering, Marmara University, Kadikoy, 34722 Istanbul, Turkey

ARTICLE INFO

Article history:
Received 20 July 2015
Accepted 5 October 2015
Available online 29 October 2015

Keywords:
Flux balance analysis
Flux distribution
Halomonas sp. AAD12
Halophilic
Principle component analysis

ABSTRACT

Background: Osmolytes with their effective stabilizing properties are accumulated as protectants not only against salinity but also against denaturing harsh environmental stresses such as freezing, drying, high temperatures, oxygen radicals and radiation. The present work seeks to understand how *Halomonas* sp. AAD12 cells redirect carbon flux specifically to replenish reactions for biomass and osmolyte synthesis under changing salinity and temperature. To accomplish this goal, a combined FBA–PCA approach has been utilized.
Results: Experimental data were collected to supply model constraints for FBA and for the verification of the model predictions, which were satisfactory. With restrictions on the various combinations of selected anaplerotic paths (reactions catalyzed by phosphoenolpyruvate carboxylase, pyruvate carboxylase or glyoxylate shunt), two major phenotypes were found. Moreover, under high salt concentrations, when the glucose uptake rate was over 1.1 mmoL DCW^{-1} h^{-1}, an overflow metabolism that led to the synthesis of ethanol caused a slight change in both phenotypes.
Conclusions: The operation of the glyoxylate shunt as the major anaplerotic pathway and the degradation of 6-phosphogluconate through the Entner–Doudoroff Pathway were the major factors in causing a distinction between the observed phenotypes.

1. Introduction

Halophilic microorganisms demand high salt concentrations to grow. They evolved two major osmoadaptation mechanisms to cope with salinity: the salt-in-cytoplasm mechanism and the organic osmolyte mechanism [1]. In the first mechanism, enzymes and structural cell components adapt to the presence of molar concentrations of KCl, and the continued presence of high salt concentrations becomes a requirement for survival. In the second mechanism, however, osmolytes are accumulated to protect the proteins, nucleic acids, biomembranes and even the whole cells against denaturation, inactivation, and inhibition. The design of the cell's interior remains basically unaltered [2]. As a response to changing external salinity, these organisms adjust their cytoplasmic osmolyte pools by remodeling their metabolism to redirect carbon flux [3,4,5,6]. Interestingly, osmolytes have been reported to be beneficial not only as osmoregulatory solutes but also as protectants against the denaturing environmental stresses of harsh environments such as freezing, drying, high temperatures, oxygen radicals and even radiation [7,8,9,10]. They possess powerful stabilizing properties that are explained by the osmophobic effect [11].

Constraint-based metabolic network modeling (CBM) methods are powerful tools that can be used to elucidate the metabolic responses of microorganisms to environmental conditions. Among the many CBMs, optimality-based flux balance analysis (FBA) is a powerful tool to simulate and study the flux distributions of the cellular metabolism [12]. FBA results can be utilized for the interpretation and prediction of distinct patterns of metabolic pathway utilization in a phenotypic and functional context [13,14]. An FBA study can be enhanced by the integrated use of statistical analysis methods such as principle component analysis (PCA). As proposed by Liang et al. [15], a combined FBA–PCA approach can not only help gain insight into the cellular metabolism of the microorganism but also enable the identification of key reactions that affect phenotypic responses of the cells to environmental conditions.

The combined FBA–PCA approach involves running *in silico* experiments, with each experiment represented as a solution to an FBA problem. In the present work, for *Halomonas* sp. AAD12 cells, the effects of the environmental conditions, salinity and temperature, and the resulting phenotypic responses are introduced into the FBA problems via constraints on fluxes such as oxygen and glucose uptake and osmolyte synthesis rates, the values of which are acquired experimentally under relevant conditions. The optimality condition for

* Corresponding author.
E-mail address: alpagu.sayar@marmara.edu.tr (N.A. Sayar).
Peer review under responsibility of Pontificia Universidad Católica de Valparaíso.

http://dx.doi.org/10.1016/j.ejbt.2015.09.010

all *in silico* experiments is maximal growth. The results of the *in silico* experiments (series of flux distributions) are then statistically analyzed using PCA to identify the key reactions that give rise to metabolic patterns. PCA is a statistical method that is commonly used for dimension reduction in high-dimensional data sets to identify the directions of largest variation [16].

2. Materials and methods

2.1. Bacterial strains and chemicals

The chemicals used were supplied by Merck AG (Darmstadt, Germany) and Sigma Chem. Ltd. (USA). The *Halomonas* sp. strain AAD12 was isolated from salt sediments in ponds found in the Çamalti Saltern area in Izmir (western Turkey) and identified as described previously [17,18]. The organism is deposited at our research laboratory at Marmara University, and its 16S rRNA sequence has been deposited in the NCBI database with the accession no. GU397429 [17]. No specific permissions were required for the collection of the samples because no endangered or protected species were involved during the field studies.

2.2. Calculation of the growth rate and glucose uptake rate

Cells were cultured at 180 rpm in 250 or 500 mL flasks containing 50 or 100 mL of M9 minimal medium, respectively. The growth medium was supplemented with 5 or 15% sodium chloride and 0.5% (w/v) glucose as the carbon source. Growth was achieved at both 37°C and 20°C. The growth was monitored spectrophotometrically at OD 600 nm. Values from triplicate measurements were averaged.

To calculate the glucose uptake rate in the presence of 5% NaCl at 37°C, 1 mL samples from actively growing cultures were taken at different time intervals during the exponential growth phase. Following centrifugation, the cell-free supernatants were analyzed by HPLC (Agilent Technologies, USA) to quantify the residual glucose in the growth media using an Agilent ZORBAX CARBOHYDRATE column. The values obtained were used to calculate the amount of glucose that was consumed. The glucose uptake rate was found by dividing the amount of glucose consumed per gram dry cell in a given period by the duration of that period.

2.3. Construction of the FBA model

FBA methodology was selected to investigate the metabolic network of *Halomonas* sp. AAD12. The input information required for FBA analysis comprises the metabolic network of the microorganism, glucose uptake rate, oxygen transfer rate, and osmolyte synthesis rates. The minimal network, which consisted of the central carbon metabolism and the pathways for the measured osmolytes, was based on the genome data of *Halomonas elongata* and on the information for *Chromohalobacter salexigens* in the KEGG database [2,19]. Reactions with no impact on the central biological topic being addressed have been excluded. The related 82 reactions were compiled in a stoichiometric matrix with a total of 88 metabolites [20]. Biomass formulation was based on the composition of *Escherichia coli* synthesized from 13 precursor metabolites with modifications to account for variations in the halophiles. The details of the biomass formulation for the high and low salt cases are given elsewhere [20].

The experimentally obtained values in this study for the glucose uptake rate were used as input constraints in flux analysis. The upper limits for the approximate oxygen uptake rates for the low and high salt cases were taken to be 2.675 and 1.175 mmoL DCW^{-1} h^{-1}, respectively. These numbers were obtained from a previous study that was conducted in 500 mL fermentors at 37°C. Because there were no measurements at 20°C, the same upper limits were assumed for the low temperature cases. Experimental data for the amounts of the three osmolytes, ectoine, hydroxyectoine and proline, in *Halomonas* sp. AAD12 cytoplasm in the early exponential and mid-exponential phases, were obtained from Dilek Kazan (personal communication, unpublished data). One assumption that was made to complete the necessary input information for FBA was related to the consumption of glucose at various growth conditions: 50% of the initially available glucose was assumed to be consumed by the growing culture between the early exponential and mid-exponential phases. Because these time points also coincided with sampling for osmolyte measurements, this choice was a reasonable assumption. Moreover, HPLC measurements also confirmed that this assumption was valid for the case of growth in the presence of 5% NaCl at 37°C.

2.4. In silico experimentation

To elucidate the possible distinct patterns of *Halomonas* sp AAD12 metabolism, 5 case studies were devised. Each case study was designed to study the flux distributions when certain metabolic pathways of the minimal network were restricted. The first case study had no restrictions imposed, while case studies 2, 3 and 4 had restrictions on the anaploretic paths: reactions catalyzed by phosphoenolpyruvate carboxylase, pyruvate carboxylase or glyoxylate shunt, respectively. For case 5, the reactions that were catalyzed by both phosphoenolpyruvate carboxylase and pyruvate carboxylase were restricted.

The conditions for the *in silico* investigation were chosen in parallel to the conditions that the available experimental data were acquired: low and high salinity conditions each at 20°C and 37°C growth temperatures giving rise to a four-by-four experimental design space. The independent variable to be examined was the glucose uptake rate, which was varied between 0.1 and 1.5 mmoL DCW^{-1} h^{-1} by 0.1 increments resulting in a maximum of 75 *in silico* experiments for each case mentioned.

The flux distributions for 82 intracellular metabolic reactions for each set of experimentation were analyzed using PCA to identify the key reactions that govern the observed metabolic patterns. The *in silico* experimental results were inserted into a data matrix in which each column corresponds to a flux vector under a specific condition and each row corresponds to the fluxes of a specific reaction under different conditions.

3. Results

3.1. Growth and glucose consumption under different salinities and temperatures

Growth of *Halomonas* sp. AAD12 has been investigated at 20 and 37°C in the presence of 5 and 15% NaCl. The fastest growth was at 37°C in the presence of 5% NaCl, with a growth rate of 0.1216 h^{-1} during the exponential phase. Exponential growth was approximately 20 h under these conditions. At a constant temperature, when the salinity increased to 15%, the maximum growth rate dropped to 0.0869 h^{-1}. Although the length of the exponential phase remained basically unchanged, the lag phase was approximately 3 times longer. Reducing the growth temperature to 20°C further repressed the

Table 1
Growth rate of *Halomonas* sp. AAD12 during the exponential phase under different conditions.

NaCl concentration	37°C		20°C	
	Experimental	Simulated result	Experimental	Simulated result
5%	0.12 h^{-1}	0.12 h^{-1}	0.06 h^{-1}	0.02 h^{-1}
15%	0.09 h^{-1}	0.04 h^{-1}	0.03 h^{-1}	0.01 h^{-1}

growth and increased the lag phase to almost 50 h. Maximum growth rates at 20°C with 5 and 15% NaCl were 0.0597 and 0.0347 h^{-1}, respectively (Table 1).

Glucose consumption during the exponential phase was also calculated under the same growth conditions for *Halomonas* sp. AAD12. The values obtained are summarized in Table 2. Apparently, the rates that were obtained for glucose uptake bear a high resemblance to the growth rates. The highest uptake rate was at 37°C in the presence of 5% NaCl, and the lowest uptake rate was at 20°C in the presence of 15% NaCl. Lowering the growth temperature and increasing the salt concentration restricted the glucose utilization, as reflected in the growth rate.

3.2. Osmolyte synthesis under changing salinity and temperature

The major osmolytes that are synthesized by *Halomonas* sp. AAD12 under osmotic pressure were previously found to be the amino acid proline and the amino acid derivatives ectoine and hydroxyectoine [20]. Hence, from the available data on the intracellular accumulation of proline, ectoine and hydroxyectoine, synthesis rates for these osmolytes at 37 and 20°C have been calculated, and the results are presented in Table 3.

At 37°C, the rate of ectoine synthesis was higher when compared to the rates at 20°C; however, with increasing salinity, the rate dropped significantly. A similar trend in the synthesis rate has also been observed for proline. Interestingly, only for hydroxyectoine, the synthesis rate increased with increasing salinity at 37°C. Surprisingly, for all three osmolytes, the synthesis rates were extremely low at 20°C.

3.3. Distribution of major fluxes under the experimental conditions investigated

The experimental values for the glucose uptake, maximum oxygen transfer and osmolytes' syntheses during the growth of *Halomonas* sp. AAD12 have been used as model constraints to perform flux balance analysis with the aim of understanding the distribution of the carbon source under different salinities and temperatures in this microorganism. For the four conditions that were investigated, the simulation results for the growth rates were consistent with the experimentally obtained values (Table 1). Both an increase in salinity and a decrease in temperature slowed down the rate of growth. The bacterial growth rate of the simulated microorganism was fixed by the upper limit of the glucose uptake rate, which had been experimentally determined. Biomass production per mole of glucose utilized remained constant regardless of the changing environmental stress.

Numerical values that were obtained for the oxygen uptake rate are presented in Table 4. The upper limits for the maximum oxygen uptake rates had been introduced into the FBA analysis as constraints. The calculations showed that a decrease in the temperature and an increase in the salinity were accompanied with reduced oxygen uptake rates. This decrease was very sharp; specifically at 37°C, the salinity increased from 5 to 15%. Nevertheless, this finding appeared to be correlated with the drop in the growth rates and glucose uptake rates. Hence, in addition to the glucose requirement, the oxygen requirement per gram cell was also constant.

Table 3
Osmolyte synthesis rate (mmoL $gDCW^{-1}$ h^{-1}) of *Halomonas* sp. AAD12.

Temperature	NaCl concentration	Ectoine	Hydroxyectoine	Proline
37°C	5%	0.0895	0.0003	0.0322
	15%	0.0106	0.0049	0.0080
20°C	5%	0.0003	0.00004	0.0004
	15%	0.0001	0.00001	0.0001

Key features of the flux distributions that are common to the four cases can be outlined as follows:

- Glycolysis operated in the forward direction for glucose degradation. However, the majority of glucose-6-phosphate that was synthesized in the initial step of glycolysis (>83%) was diverted to the pentose phosphate pathway. Major fructose-6-phosphate demand for glycolysis and biomass was met by synthesis through the non-oxidative branch of the pentose phosphate pathway. Extra glyceraldehyde synthesized through the pentose phosphate pathway was also recycled to glycolysis. There was considerably high flux through the pentose phosphate pathway. Both the oxidative and non-oxidative branches were active in the forward direction for the synthesis of precursor metabolites and the cofactor NADPH. The flux through the final alternative path for glucose degradation, the Entner–Doudoroff Pathway, was negligibly small.
- There was significant flux through the anaplerotic pathways. Approximately 15% of the phosphoenolpyruvate and 20% of the pyruvate that was synthesized in glycolysis was directed to oxaloacetate synthesis to replenish the missing precursors in all of the four cases. In general, an increase in the salinity increased the flux to these replenishing reactions by 1–2%, at both 20 and 37°C. Flux through the glyxoylate shunt remained negligibly small under these experimental conditions. Anaplerosis was mainly achieved by pyruvate carboxylase and phosphoenolpyruvate carboxylase

3.4. Phenotypic analysis of the Halomonas sp. strain AAD12 under changing glucose utilization

Having established a minimal metabolic model of *Halomonas* sp. AAD12 using FBA, with experimental and simulated values agreeing to a satisfactory extent, the model could be used to perform *in silico* experimentation to study the phenotypic responses of the microorganism to changing nutritional conditions. Keeping the rates of the osmolyte synthesis constant, a topological analysis has been performed for the four growth conditions under study to investigate the redistribution of glucose among the anaplerotic reactions because many precursor metabolites were drained from the system for biomass and osmolyte synthesis. The assumption in keeping with the osmolyte synthesis rates being constant is that under the studied conditions, the halophilic *Halomonas* sp. AAD will prioritize the synthesis of osmolytes in the appropriate amounts to protect itself against the thermo-saline conditions of the environment by reorganizing its metabolic flux distribution depending on the amount of nutrition (glucose) available. For this reason, the glucose rate uptake was allowed to vary from 0.1 to 1.5 mmoL DCW^{-1} h^{-1} on 0.1 increments. The main focus was on three major paths: the

Table 2
Glucose uptake rate of *Halomonas* sp. AAD12.

NaCl concentration	v_{Glu} (mmoL DCW^{-1} h^{-1})	
	37°C	20°C
5%	1.16	0.19
15%	0.35	0.09

Table 4
Simulated results for the oxygen uptake rate of *Halomonas* sp. AAD12.

NaCl concentration	v_{oxygen} (mmoL DCW^{-1} h^{-1})	
	37°C	20°C
5%	1.18	0.21
15%	0.37	0.10

Table 5
Cases investigated for glucose redirection to anaplerotic pathways.

	Inactive enzyme or pathway
Case 1	–
Case 2	Phosphoenolpyruvate carboxylase
Case 3	Pyruvate carboxylase
Case 4	Glyoxylate shunt
Case 5	Phosphoenolpyruvate carboxylase and pyruvate carboxylase

glyoxylate shunt and the synthesis of oxaloacetate from pyruvate or phosphoenolpyruvate. The five cases for the four conditions compared are summarized in Table 5.

The simulations showed that the sum of the fluxes through the selected anaplerotic pathways remained constant at a constant glucose uptake rate, as long as the oxaloacetate was replenished from pyruvate and/or phosphoenolpyruvate. When oxaloacetate synthesis from pyruvate was not possible, replenishment was achieved through synthesis mainly from phosphoenolpyruvate or vice versa. Flux through the glyoxylate shunt remained negligible unless it was the only anaplerotic pathway.

The application of principal component analysis to these flux distributions revealed two distinct phenotypes under each growth condition. The phenotypes observed are summarized in Table 6. One phenotype was observed (F1a–F1d) when there was oxaloacetate formation from pyruvate and/or phosphoenolpyruvate (cases 1–4), and the other phenotype (F2a–F2d) was observed when only the glyoxylate shunt was active as the sole anaplerotic pathway (case 5) (Fig. 1a–Fig. 1d).

As long as there is sufficient oxaloacete formation from pyruvate and/or phosphoenolpyruvate (cases 1–4), there was no significant variation within and between the phenotypes F1b, F1c, and F1d at different glucose uptake rates that were below 1.1 mmoL DCW^{-1} h^{-1}. Above the glucose uptake rates of 1.1 mmoL DCW^{-1} h^{-1}, another minor phenotype emerged at a high salt concentration (within the phenotypes F1b and F1d, Fig. 1b and Fig. 1d). Moreover, regardless of the change in temperature, these new phenotypes were also similar. This change in the phenotypes was indicated by a kink/bent on the scores plot that corresponds to the first two PCs from the PCA. Interestingly, the phenotype observed during growth at 37°C with 5% NaCl (F1a) was totally different from the other F1 phenotypes.

An identical trend was obtained within the F2 phenotypes when only the glyoxylate shunt was active as an anaplerotic pathway. Apart from those subjected to growth at 37°C with 5% NaCl, cells with different glucose uptake rates below 1.1 mmoL DCW^{-1} h^{-1} were phenotypically similar. However, further increasing the glucose uptake rate resulted in the emergence of a new phenotype, similar to in the F1 phenotypes.

Based on metabolic flux distributions, there exist a couple of major differences between the F1 and F2 phenotypes, which cause the following distinction:

(1) Flux through glycolysis is significantly lower in cells with F2 phenotypes.
(2) The pentose phosphate pathway preferably runs in the reverse direction in cells with F2 phenotypes.
(3) The Entner–Doudoroff Pathway is frequently active in F2 cells, specifically when the pentose phosphate pathway operates in the reverse direction.
(4) Flux through the Krebs cycle is higher in the F2 phenotypes, which is probably due to the synthesis of glyoxylate.
(5) The oxygen demand of the F2 phenotypes is higher.

Table 6
Phenotypes of *Halomonas* sp. strain AAD12.

Simulation	Phenotype
5% NaCl & 37°C, cases 1–4	F1a
15% NaCl & 37°C, cases 1–4	F1b
5% NaCl & 20°C, cases 1–4	F1c
15% NaCl & 20°C, cases 1–4	F1d
5% NaCl & 37°C, case 5	F2a
15% NaCl & 37°C, case 5	F2b
5% NaCl & 20°C, case 5	F2c
15% NaCl & 20°C, case 5	F2d

4. Discussion

Certain amino acids and their derivatives, such as proline, glutamate, ectoine, and betaine are typically accumulated as osmolytes in halophilic and halotolerant bacteria as a response to changes in salinity to keep proteins in their natively folded structures. The osmophobic property of the osmolytes enables proteins to counter-balance the perturbations of salinity that lead to the avoidance of changes in the secondary and tertiary structures [9]. While these osmolytes are commonly reported to be increasing the thermodynamic stability of the proteins against salt stress, selected reports hint that these osmolytes also render thermostability to the enzymes [21,22]. Indeed, the expression and roles of osmolytes during heat stress have been investigated by García-Estepa et al. [23] and Reina-Bueno et al. [24] in *C. salexigens* and by Bursy et al. [25] in *Streptomyces coelicolor* A3(2). These results clue that the regulation of the osmolyte synthesis involves a highly complex mechanism that involves the interconnected action of signaling, regulatory and metabolic networks.

The compounds synthesized by *Halomonas* sp. AAD12 in complex medium under salt stress have been reported to be proline, ectoine and hydroxyectoine [20]. The precursor metabolite for the synthesis of proline is alpha-ketoglutarate, whereas the ectoine syntheses consume oxaloacetate. This arrangement means that in addition to the requirement for biomass synthesis, two intermediates of the tricarboxylic acid (TCA) cycle are continuously drained from the cyclic pathway in significant amounts for osmolyte synthesis. Consequently, the missing metabolites should be replenished through anaplerotic reactions because the TCA cycle could be considered to be the hub of the metabolism for energy production and biosynthetic reactions. When there are osmotic and temperature stresses, however, how does *Halomonas* sp. AAD12 redirect the available glucose to the replenishing reactions? To address this question, the synthesis of oxaloacetate either from pyruvate or phosphoenolpyruvate and the conversion of acetyl-coA to succinate through the glyoxylate shunt were regarded as possible targets of the regulatory control over the minimal metabolic network that is constructed for *Halomonas* sp. AAD12. This minimal metabolic network comprises the important metabolic pathways that could give rise to phenotypic variance through different flux distributions. However, the signaling and regulatory networks are not represented.

Under salinity and/or thermal stress, the rate of osmolyte synthesis in *Halomonas* sp. AAD12 changed significantly as a part of the protection mechanism. As the osmolyte synthesis rates increased or decreased, the variation among the fluxes was not systematic. Nevertheless, the behavior of the microorganism was phenotypically similar under the experimental conditions that were investigated. As the glucose uptake rate dropped with increasing salinity or decreasing temperature, fluxes in general also dropped in the major catabolic pathways: glycolysis, pentose phosphate pathway and TCA cycle. Ceylan et al. [20] also reported that the rate of catabolic reactions slowed down significantly with increasing salinity. Moreover, they have supported this finding by protein expression data. Interestingly, the drop reported for fluxes of *Halomonas* sp. AAD12 in this work was slightly higher in the glycolytic pathways but was slightly lower in the pentose phosphate pathway, which indicated that under salinity and/or thermal stress, the pentose phosphate pathway could be more

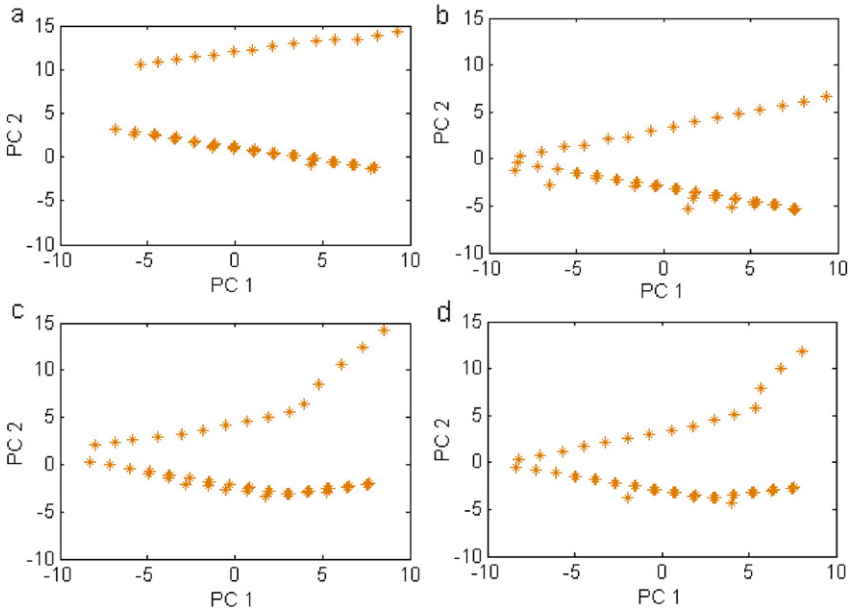

Fig. 1. PCA analysis of *in silico* experimentation results. Sub plot a: 5% NaCl, 37°C; b: 5% NaCl, 20°C; c: 15% NaCl, 37°C; and d: 15% NaCl, 20°C.

favorable over glycolysis. This preference could be dictated by the reduced cofactor and energetic requirements of the microorganism.

The distribution of the osmolytes hence the fluxes were totally different when the same microorganism used citrate as its major carbon source under changing salinity [20]. In contrast to the flux distributions obtained in this work, Ceylan et al. [20] reported that the high fluxes centered around the TCA cycle at both low and high salinity and the directionality of the net reactions were variable. Overall, rather than glycolysis, gluconeogenesis was active. This difference was expected because the carbon breakdown started in the TCA cycle.

Flux analysis using the experimental conditions used showed that anaplerosis in *Halomonas* sp. AAD12 was mainly achieved by the actions of pyruvate carboxylase and phosphoenolpyruvate carboxylase but not through the glyoxylate shunt. Both carboxylases are parts of carbon fixation reactions that give TCA cycle intermediates, whereas the glyoxylate shunt is a modified form of the TCA cycle. The glyoxylate shunt bypasses the reactions of the TCA cycle in which carbon dioxide is released, conserving 4-carbon compounds of biosynthetic reactions. Because it is usually active when growth on 2-carbon compounds requires conservation of 4-carbon TCA cycle intermediates, expectedly it was not the primary anaplerotic reaction in *Halomonas* sp. AAD12.

The next phase of analysis involved performing *in silico* experimentation to study the phenotypic responses of the microorganism to changing nutritional conditions that impose the same stresses. We have chosen the above-mentioned three anaploretic paths as possible targets of the regulatory control over the minimal metabolic network.

The plot of the scores that correspond to the first two PCs from the PCA of the *in silico* results identified two phenotypes. Pathway analysis noted that the distinction between these phenotypes was based on three major factors:

(1) *The presence of the glyoxylate shunt as the major anaplerotic pathway that indirectly influences the extent to which the TCA cycle is utilized*
There are two intermediates of the TCA cycle that are consumed in biosynthetic reactions and for osmolyte synthesis: oxaloacetate and alpha-ketogluterate. When oxaloacetate was replenished over pyruvate and/or phosphoenolpyruvate, the TCA cycle terminated at alpha-ketogluterate because there was no requirement for the synthesis of the other TCA cycle intermediates. When the glyoxylate shunt was the sole anaplerotic path, alpha-ketogluterate was still the terminal intermediate of the TCA cycle. However, this time, the synthesis of glyoxylate forced the TCA cycle to operate from succinate to oxaloacetate.

(2) *The fate of 6-phosphogluconate, which could be consumed through either the pentose phosphate pathway or Entner–Doudoroff Pathway*
The 6-phosphogluconate consumption route determined how the precursors of biosynthetic reactions such as ribose-5-phosphate and erythrose-4-phosphate were synthesized. When 6-phosphogluconate was converted to ribulose-5-phospate through the oxidative branch of the pentose phosphate pathway, the non-oxidative branch of the pentose phosphate pathway operated in the forward direction. When 6-phosphogluconate entered the Entner–Doudoroff Pathway, the requirements for ribose-5-phosphate and erythrose-4-phosphate were met by the pentose phosphate pathway running in the reverse direction. Metabolites to initiate the synthesis of ribose-5-phosphate and erythrose-4-phosphate (*i.e.*, glyceraldehyde-3-phosphate and fructose-6-phosphate) were drained from glycolysis.
Interestingly, when the fluxes through all of the anaplerotic pathways were relaxed, the flux through the glyoxylate shunt was always negligible, and the Entner–Doudoroff Pathway was inactive. What dictates the preference for the Entner–Doudoroff Pathway? Usually, the Entner–Doudoroff Pathway was active when the glyoxylate shunt was the sole anaplerotic path. However, this point requires further attention.

(3) *The synthesis of ethanol that was triggered at glucose uptake rates above 1.1 mmoL DCW^{-1} h^{-1} in the presence of high salt concentration*
In the presence of a high salt concentration, regardless of the difference in temperature, the microorganism could not avoid overflowing metabolism at high glucose uptake rates under all of the conditions studied. Consequently, ethanol formed as a side metabolite, which led to a change in the phenotype.
The minor differences in the metabolic paths due to changes in the directionality of the reactions, such as conversion of glucose-6-phosphate to fructose-6-phosphate or conversion of phosphoenolpyruvate to pyruvate, were not alone sufficient to lead to variations in the phenotypes.

5. Conclusions

In this work, a combined FBA–PCA approach was used to study the adaptation through redirected carbon flux of the halophilic microorganism *Halomonas* sp. AAD12 to different salinities and temperatures using a reconstructed minimal metabolic network. Experimental data were collected to supply model constraints for FBA and for verification of the model predictions that were satisfactory. The model was subsequently used to conduct *in silico* experiments under varying glucose uptake rates. The results of the *in silico* experiments were analyzed using PCA to identify probable phenotypes that arose due to redirected flux distributions. The utilization patterns of the anaplerotic reactions pointed to two major phenotypes. Under a high salt concentration and high glucose uptake rates, the overflow metabolism that led to the synthesis of ethanol caused a change in both phenotypes.

The combined FBA–PCA approach is potentially a powerful tool for the interpretation of metabolic network models using *in silico* experiments. Preliminary inferences can be made about the metabolism of a microorganism for which there is relatively scarce information and a limited amount of wet experimentation. Initial hypothesis forming and testing can also be reinforced by the use of this approach. However, the model assumptions must be made and interpreted with utmost care. Similarly, the design of the *in silico* experiments must be made appropriately to derive the relevant results.

The current study uses a minimal metabolic network and a manageable *in silico* experimental design that allows the manual inspection and interpretation of the flux distribution results. However, considering that the same approach can be applied to genome-scale metabolic network models and a wider *in silico* experimental design space, there is a need for a computational tool that integrates expert knowledge, heuristics and statistical analysis. Integrating the FBA–PCA approach with such a tool would be a potentially interesting direction for future work.

References

[1] Oren A. Halophilic microorganisms and their environments. Dordrecht: Kluwer Academic Publishers; 2002.

[2] Schwibbert K, Marin-Sanguino A, Bagyan I, Heidrich G, Lentzen G, Seitz H, et al. A blueprint of ectoine metabolism from the genome of the industrial producer *Halomonas elongata* DSM 2581(T). Environ Microbiol 2011;13:1973–94. http://dx.doi.org/10.1111/j.1462-2920.2010.02336.x.

[3] Bremer E, Kramer R. Coping with osmotic challenges: Osmoregulation through accumulation and release of compatible solutes in bacteria. In: Storz G, Hengge-Aronis R, editors. Bacterial stress responses. Washington DC: ASM Press; 2000. p. 77–97.

[4] Empadinhas N, da Costa MS. Osmoadaptation mechanisms in prokaryotes: Distribution of compatible solutes. Int Microbiol 2008;11:151–61.

[5] Galinski EA, Trüper HG. Microbial behaviour in salt-stressed ecosystems. FEMS Microbiol Rev 1994;15:95–108. http://dx.doi.org/10.1111/j.1574-6976.1994.tb00128.x.

[6] Vargas C, Argandoña M, Reina-Bueno M, Rodríguez-Moya J, Fernández-Aunión C, Nieto JJ. Unravelling the adaptation responses to osmotic and temperature stress in *Chromohalobacter salexigens*, a bacterium with broad salinity tolerance. Saline Syst 2008;4:14. http://dx.doi.org/10.1186/1746-1448-4-14.

[7] Borges N, Ramos A, Raven ND, Sharp RJ, Santos H. Comparative study of the thermostabilizing properties of mannosylglycerate and other compatible solutes on model enzymes. Extremophiles 2002;6:209–16. http://dx.doi.org/10.1007/s007920100236.

[8] Kumar R. Role of naturally occurring osmolytes in protein folding and stability. Arch Biochem Biophys 2009;491:1–6. http://dx.doi.org/10.1016/j.abb.2009.09.007.

[9] Lippert K, Galinski EA. Enzyme stabilization by ectoine type compatible solutes: Protection against heating, freezing and drying. Appl Microbiol Biotechnol 1992; 37:61–5. http://dx.doi.org/10.1007/BF00174204.

[10] Pastor JM, Salvador M, Argandoña M, Bernal V, Reina-Bueno M, Csonka LN, et al. Ectoines in cell stress protection: Uses and biotechnological production. Biotechnol Adv 2010;28:782–801. http://dx.doi.org/10.1016/j.biotechadv.2010.06.005.

[11] Bolen DW, Baskakov IV. The osmophobic effect: Natural selection of a thermodynamic force in protein folding. J Mol Biol 2001;310:955–63. http://dx.doi.org/10.1006/jmbi.2001.4819.

[12] Raman K, Chandra N. Flux balance analysis of biological systems: Applications and challenges. Brief Bioinform 2009;10:435–49. http://dx.doi.org/10.1093/bib/bbp011.

[13] Bordbar A, Monk JM, King ZA, Palsson BO. Constraint-based models predict metabolic and associated cellular functions. Nat Rev Genet 2014;15:107–20. http://dx.doi.org/10.1038/nrg3643.

[14] Edwards JS, Ramakrishna R, Palsson BO. Characterizing the metabolic phenotype: A phenotype phase plane analysis. Biotechnol Bioeng 2002;77:27–36. http://dx.doi.org/10.1002/bit.10047.

[15] Liang M, He QP, Jeffries TW, Wang J. Elucidating xylose metabolism of *Scheffersomyces stipitis* by integrating principal component analysis with flux balance analysis. Am Control Conf 2013:3777–82. http://dx.doi.org/10.1109/ACC.2013.6580415.

[16] Abdi H, Williams LJ. Principle component analysis. Wiley Interdiscip Rev Comput Stat 2010;2:433–59. http://dx.doi.org/10.1002/wics.101.

[17] Ceylan S, Sariyar-Akbulut B, Denizci AA, Kazan D. Proteomic insight into phenolic adaptation of a moderately halophilic *Halomonas* sp. strain AAD12. Can J Microbiol 2011;57:295–302. http://dx.doi.org/10.1139/w11-009.

[18] Sariyar-Akbulut B. Discriminant function analysis based on principal components for rapid discrimination of metabolic capabilities of new isolates. Chem Biochem Eng Q 2010;24:119–27.

[19] Kanehisa M, Goto S. KEGG: Kyoto encyclopedia of genes and genomes. Nucleic Acids Res 2000;28:27–30. http://dx.doi.org/10.1093/nar/28.1.27.

[20] Ceylan S, Yilan G, Sariyar-Akbulut B, Poli A, Kazan D. Interplay of adaptive capabilities of *Halomonas* sp. AAD12 under salt stress. J Biosci Bioeng 2012;114: 45–52. http://dx.doi.org/10.1016/j.jbiosc.2012.02.030.

[21] Wang YB, Nagata S. Participation of ions and solutes on the thermostability of alpha-amylase. Chin J Biotechnol 2004;20:104–10.

[22] Zhang L, Wang Y, Zhang C, Wang Y, Zhu D, Wang C, et al. Supplementation effect of ectoine on thermostability of phytase. J Biosci Bioeng 2006;102:560–3. http://dx.doi.org/10.1263/jbb.102.560.

[23] García-Estepa R, Argandoña M, Reina-Bueno M, Capote N, Iglesias-Guerra F, Nieto JJ, et al. The *ectD* gene, which is involved in the synthesis of the compatible solute hydroxyectoine, is essential for thermoprotection of the halophilic bacterium *Chromohalobacter salexigens*. J Bacteriol 2006;188:3774–84. http://dx.doi.org/10.1128/JB.00136-06.

[24] Reina-Bueno M, Argandon M, Salvador M, Rodriguez-Moya J, Iglesias-Guerra F, Csonka LN, et al. Role of trehalose in salinity and temperature tolerance in the model halophilic bacterium *Chromohalobacter salexigens*. PLoS One 2012;7:e33587. http://dx.doi.org/10.1371/journal.pone.0033587.

[25] Bursy J, Kuhlmann AU, Pittelkow M, Hartmann H, Jebbar M, Pierik AJ, et al. Synthesis and uptake of the compatible solutes ectoine and 5-hydroxyectoine by *Streptomyces coelicolor* A3(2) in response to salt and heat stresses. Appl Environ Microbiol 2008; 74:7286–96. http://dx.doi.org/10.1128/AEM.00768-08.